

Gravitational Waves of GUT Phase Transition during Inflation

Xi-He Hu^{a,b,c} and Ye-Ling Zhou^a

^a*School of Fundamental Physics and Mathematical Sciences, Hangzhou Institute for Advanced Study, UCAS, Hangzhou 310024, China*

^b*Institute of Theoretical Physics, Chinese Academy of Sciences, Beijing 100190, China*

^c*University of Chinese Academy of Sciences, Beijing 100049, China*

E-mail: huxihe23@mailsucas.ac.cn, zhouyeling@ucas.ac.cn

ABSTRACT: GUT phase transition during inflation solves the GUT monopole problem on one hand. On the other hand, gravitational waves (GWs) from such a phase transition, if it is first-order, are redshifted and deformed, and might be observed today in GW observatories. We review the formalism of inflated GWs and derive the general deformation function between inflated and uninflated GW spectra in the instant-source application. It is valid for any e-folding number of instant source. Applying the formalism to GUT phase transition, we find that the e-folding number at 15 or 25 can shift the GWs to 10 Hz or mHz hands, respectively, which might be tested in the future ground-based or space-based interferometers. We further generalise the discussion to inflated GWs via phase transition below the GUT scale. It is worth mentioning that, due to the deformation of the spectrum, the peak of inflated GWs is not simply a redshift of the peak of uninflated GWs.

Contents

1	Introduction	1
2	General formulation of inflated GWs	2
2.1	Production and propagation of GWs	2
2.2	Inflated GW spectrum in the instant-source approximation	5
2.3	IR and UV behaviour of the inflated GW spectrum	8
3	Application to GUT phase transition	10
3.1	Solution to the monopole problem	10
3.2	Inflated GWs via GUT phase transition	11
3.3	Inflated GWs via phase transition below GUT scale	16
4	Conclusions	17

1 Introduction

Grand Unified Theories (GUTs) possess exactly large gauge symmetries that mix the strong and electroweak interactions, and the symmetries become spontaneously broken at an exceedingly high energy scale, the GUT scale. The existence of magnetic monopoles is a universal prediction in GUTs, in spite of the detail of GUT symmetry breaking [1, 2]. Monopoles have masses in general of the same order of the GUT scale. They cause cosmological problem if they are generated in the radiation era, since their energy density remaining today exceeds the critical energy density of the Universe too much. Embedding an inflationary era before the radiation era and spontaneously breaking GUT symmetry before or during inflation dilute the monopole number density and thus provide an appealing solution to the GUT monopole problem [3–5].

GWs have been suggested as a complementary probe to GUTs along with proton decay measurements [6]. It utilises the property of $SO(10)$ GUTs that $SO(10)$ contains the gauged $U(1)_{B-L}$ sub-symmetry, and GWs are emitted from cosmic strings, which are generated after the spontaneous breaking of $U(1)_{B-L}$ [7]. The $U(1)_{B-L}$ symmetry breaking scale is in general split away from the GUT scale, in particular in the non-SUSY model [8], and connected with the GUT scale via gauge unification [9–11]. In SUSY GUTs, these two scales might be located nearby with inflation arranged properly [12], and GWs reduced in the IR band from metastable cosmic strings are expected [13–15], seeing also in [16–19].

GWs via cosmological phase transition are motivated in the GUT framework. Specific examples have been carried out in the Pati-Salam models [20–22] and left-right symmetric models [23, 24]. To achieve a GW spectrum within the reach of GW observatories such as LIGO/Virgo/KAGRA, a relatively low intermediate scale $\sim 10^4 - 10^6$ GeV should be

satisfied, which requires appropriate threshold effects in the gauge unification [20, 22]. The property of GWs via phase transition during inflation was studied in [25]. They pointed out that GWs get redshifted by the inflation, and its power spectrum oscillates with its wave number, making itself distinct from GWs from phase transitions after the inflation. Further developments of the formalism and its applications are found in [26, 27].

In the present work, we will consider the GUT phase transition proceeds during the inflation at a certain point with e-folding number N_* . Different from some well-known inflation models, e.g., [28, 29], where the GUT breaking associates with inflationary dynamics, we will assume that the inflation evolves independent from the GUT breaking, and the GUT phase transition is carried out very fast. In such a case, the phase transition will be regarded as an instant source of GW production, and the inflaton field is simply a background during the phase transition.

The rest of this paper is organised as follows. In section 2, we review the formalism of GWs via phase transition during inflation. A more general formalism, compared with that in [25, 26], for the deformation function between the inflated GWs and the uninflated GWs (i.e., GWs via phase transition after inflation) is derived. It is valid for any value of the e-folding number $0 < N_* \lesssim 60$. We will further obtain the simplified form of the deformation function in the IR and UV regimes. We apply the formalism to GUT phase transition in section 3. We start with the appropriate regime of N_* in solving the GUT monopole solution and then concentrate on the property of inflated GWs via GUT phase transition and their testability in GW observatories. Generalisation to phase transition below the GUT scale is given in the end of the section. We conclude in section 4.

2 General formulation of inflated GWs

In this section, we will give a general review on the GWs produced from an instant source during inflation and their propagation to today. We work in the standard picture that the universe begins with an inflation (Inf) period and follows with three eras in the Λ CDM model, i.e., radiation domination (RD), matter domination (MD) and dark-energy domination (Λ D) eras. We will consider GW genesis via instant source, which happens at a certain time t_* during the inflation period. Then GWs propagate in the inflation + Λ CDM eras. During its propagation along the expansion of the Universe, the spectrum gets redshifted and deformed. We will show the formalism of the GW spectrum today from its original spectrum at production. Section 2.1 gives the formulation of EOM of GWs in the inflation. The general solution of the GW spectrum from an instant source modified by inflation is given in section 2.2. Its IR and UV behaviours are given in section 2.3.

2.1 Production and propagation of GWs

The expanding Universe in each era (Inf, RD, MD or Λ D) can be described by the Friedmann-Lemaitre-Robertson-Walker (FLRW) metric, which in the conformal frame is expressed as

$$ds^2 = a^2(\tau) [d\tau^2 - d\mathbf{x}^2] , \quad (2.1)$$

where a is the scale factor. We follow the convention $a' = \partial a / \partial \tau$, $\dot{a} = \partial a / \partial t$ with $dt = a d\tau$ understood and it is straightforward to check that the conformal Hubble factor $\mathcal{H} = a'/a$ correlates with the standard Hubble rate $H = \dot{a}/a$, as $\mathcal{H} = aH$. The conformal Hubble factor \mathcal{H} in each era (i.e., $E = \text{Inf, RD, MD and } \Lambda\text{D}$) of the Universe is given by

$$\mathcal{H}^E = \frac{1}{\tau} \times \{-1, 1, 2, -1\}, \quad (2.2)$$

respectively. Note that τ is convenient to use when studying GW dynamics in a specified era. However, it is not continuously defined when the Universe transits from the end of the last era to the beginning of the next era. When we are focusing on the the whole expanding history of the Universe, we can transform it to the co-moving factor a by default, with $a_0 = a(t_0)$ is the scale factor today.

We regard GWs as small fluctuations in the FLRW background. In the conformal coordinates, the GW metric is given by

$$ds^2 = a^2(\tau) [d\tau^2 - (\delta_{ij} + h_{ij}(\tau, \mathbf{x}))dx^i dx^j], \quad (2.3)$$

where we have considered the traceless and transverse gauge for $h_{\mu\nu}$. The motion equation of h_{ij} is written to be

$$h''_{\mu\nu}(\tau, \mathbf{x}) + 2\mathcal{H}h'_{\mu\nu}(\tau, \mathbf{x}) - \nabla^2 h_{\mu\nu}(\tau, \mathbf{x}) = 16\pi G_{\text{N}} a^2(\tau) \sigma_{\mu\nu}(\tau, \mathbf{x}), \quad (2.4)$$

where $\sigma_{\mu\nu}$ is the perturbative energy-momentum tensor of sources producing GW in the local Minkowski coordinates. Generally, one studies the spectrum of energy density of GW relying on its momentum. Therefore, we consider Fourier transforms in conformal coordinates

$$\begin{aligned} h_{ij}(\tau, \mathbf{x}) &= \int \frac{d^3 k}{(2\pi)^3} e^{-i\mathbf{k}\cdot\mathbf{x}} \tilde{h}_{ij}(\tau, \mathbf{k}), \\ \sigma_{ij}(\tau, \mathbf{x}) &= \int \frac{d^3 k}{(2\pi)^3} e^{-i\mathbf{k}\cdot\mathbf{x}} \tilde{\sigma}_{ij}(\tau, \mathbf{k}), \end{aligned} \quad (2.5)$$

and then, the equation of motion of GW in the conformal momentum space is

$$\tilde{h}''_{ij}(\tau, \mathbf{k}) + 2\mathcal{H}\tilde{h}'_{ij}(\tau, \mathbf{k}) + k^2 \tilde{h}_{ij}(\tau, \mathbf{k}) = 16\pi G_{\text{N}} a^2(\tau) \tilde{\sigma}_{ij}(\tau, \mathbf{k}). \quad (2.6)$$

We first ignore the source on the right hand side (RHS) and consider the GW propagation from an preexisting GW metric. The general solution is given by

$$\tilde{h}_{\mu\nu}(\tau, \mathbf{k}) = C_{\mu\nu,1} h_1(\tau, \mathbf{k}) + C_{\mu\nu,2} h_2(\tau, \mathbf{k}), \quad (2.7)$$

where $h_1(\tau, \mathbf{k})$ and $h_2(\tau, \mathbf{k})$ are two independent functions of Eq. (2.6) with zero source on the RHS and $C_{\mu\nu,1}$ and $C_{\mu\nu,2}$ are coefficients. In a realistic calculation, we have to specify the eras E , (for $E = \text{Inf, RD, MD, } \Lambda\text{D}$), since \mathcal{H} is different in each era. $h_1(\tau, \mathbf{k})$ and

$h_2(\tau, \mathbf{k})$ are given in different forms, as shown below

$$\begin{aligned}
h_1^{\text{Inf}}(\tau, \mathbf{k}) &= \cos k\tau + k\tau \sin k\tau, & h_2^{\text{Inf}}(\tau, \mathbf{k}) &= \sin k\tau - k\tau \cos k\tau, \\
h_1^{\text{RD}}(\tau, \mathbf{k}) &= \frac{\cos k\tau}{k\tau}, & h_2^{\text{RD}}(\tau, \mathbf{k}) &= \frac{\sin k\tau}{k\tau}, \\
h_1^{\text{MD}}(\tau, \mathbf{k}) &= \frac{\cos k\tau + k\tau \sin k\tau}{(k\tau)^3}, & h_2^{\text{MD}}(\tau, \mathbf{k}) &= \frac{\sin k\tau - k\tau \cos k\tau}{(k\tau)^3}, \\
h_1^{\text{AD}}(\tau, \mathbf{k}) &= \cos k\tau + k\tau \sin k\tau, & h_2^{\text{AD}}(\tau, \mathbf{k}) &= \sin k\tau - k\tau \cos k\tau.
\end{aligned} \tag{2.8}$$

The relevant parameters $C_{\mu\nu,1}^E$ and $C_{\mu\nu,2}^E$ are not fully free. Matching from the end of a previous era to the beginning of the next era should be taken into account. For example, h_{ij}^{Inf} at the end of inflation and h_{ij}^{RD} at the beginning of RD follows the matching conditions,¹

$$\begin{aligned}
\tilde{h}_{ij}^{\text{Inf}}(\tau, \mathbf{k})|_{\text{Rh}} &= \tilde{h}_{ij}^{\text{RD}}(\tau, \mathbf{k})|_{\text{Rh}}, \\
\partial_t \tilde{h}_{ij}^{\text{Inf}}(\tau, \mathbf{k})|_{\text{Rh}} &= \partial_t \tilde{h}_{ij}^{\text{RD}}(\tau, \mathbf{k})|_{\text{Rh}},
\end{aligned} \tag{2.9}$$

leading to the correlation among $C_{\mu\nu,1}^E$ and $C_{\mu\nu,2}^E$ between two adjacent eras. Note that the differential with respect to t in the above equation can be replaced by the differential with respect to τ if the variation of the scale factor in the reheating period is ignored.

We then solve Eq. (2.6) in the presence of a source on the RHS. The equation has a general solution expressed by the Green function,

$$\tilde{h}_{ij}(\tau, \mathbf{k}) = 16\pi G_N \int d\tau' \theta(\tau - \tau') a^2(\tau') \tilde{\sigma}_{ij}(\tau', \mathbf{k}) \mathcal{G}(\tau - \tau', \mathbf{k}), \tag{2.10}$$

where

$$\mathcal{G}(\tau - \tau', \mathbf{k}) = \left[\frac{\partial h_1}{\partial \tau} - \frac{h_1}{h_2} \frac{\partial h_2}{\partial \tau} \right]_{\tau=\tau'}^{-1} h_1(\tau, \mathbf{k}) + \left[\frac{\partial h_2}{\partial \tau} - \frac{h_2}{h_1} \frac{\partial h_1}{\partial \tau} \right]_{\tau=\tau'}^{-1} h_2(\tau, \mathbf{k}) \tag{2.11}$$

and h_1 and h_2 have been given in Eq. (2.8).

In this work, we will consider the GW is produced during the inflation, where Eq. (2.10) will be used. Once the GW is produced, its propagation in the expanding Universe follows the equation Eq. (2.7), with matching conditions between different eras, such as Eq. (2.9), to be considered.

Regarding GWs as a stochastic background, the energy density is given by

$$\rho_{\text{GW}} = \frac{1}{32\pi G_N a^2(t)} \left\langle |h'_{ij}(\tau, \mathbf{x})|^2 \right\rangle = \frac{1}{32\pi G_N a^2(t)} \int_{T_\tau} \frac{d\tau}{T_\tau} \int \frac{d^3\mathbf{k}}{(2\pi)^3 V} |h'_{ij}(\tau, \mathbf{k})|^2, \tag{2.12}$$

where V is the conformal volume. Here, the average along the relevant conformal period T_τ for GW genesis is considered. It applies in the condition that the oscillation duration is much smaller than \mathcal{H} . Thus, the energy density per logarithmic momentum in conformal coordinates is

$$\frac{d\rho_{\text{GW}}}{d \log k} = \frac{1}{64\pi^3 G_N} \frac{k^3}{V} \frac{1}{a^2(t)} \int_{T_\tau} \frac{d\tau}{T_\tau} \left| \tilde{h}'_{ij}(\tau, \mathbf{k}) \right|^2, \tag{2.13}$$

¹We remind that τ does not vary continuously during the transition from the previous era to the next era, e.g., from the end of Inf to the beginning of RD. And the matching condition here has ignored the potential modification induced by some effects during the transition.

where T_τ is duration of GW genesis in the conformal unit. The spectrum of the GW background in terms of the physical frequency f in the current epoch t_0 is defined as

$$h^2\Omega_{\text{GW}}(f) = \frac{h^2}{\rho_c} \frac{d\rho_{\text{GW}}}{d\log k} \Big|_{t=t_0, k=2\pi a_0 f}, \quad (2.14)$$

where $\rho_c = 3H_0^2/(8\pi G_N)$ is critical energy density today.

2.2 Inflated GW spectrum in the instant-source approximation

In this subsection, we approximate the GW source as an instant source and calculate the resulting GW spectrum. This approach applies to the case that the GW production is much faster than the Hubble expansion.

We fix the instant source at time τ_\star in the inflationary era, i.e.,

$$\tilde{\sigma}_{\mu\nu}(\tau, \mathbf{k}) = \frac{\delta(\tau - \tau_\star)}{a(\tau_\star)} \tilde{\sigma}_{\mu\nu}(\mathbf{k}). \quad (2.15)$$

It is convenient to obtain the Green function in Eq. (2.11) (with $E = \text{Inf}$) from time τ_\star to τ ($\tau > \tau_\star$) as

$$\mathcal{G}_{\text{Inf}}(\tau - \tau_\star, \mathbf{k}) = \frac{1}{k^2\tau_\star} \left[1 - \frac{a(\tau_\star)}{a(\tau)} \right] \cos[k(\tau - \tau_\star)] + \frac{1}{k} \left[\frac{1}{k^2\tau_\star^2} + \frac{a(\tau_\star)}{a(\tau)} \right] \sin[k(\tau - \tau_\star)], \quad (2.16)$$

where τ_\star can be expressed in terms of a_\star as $\tau_\star = -(H_\star a_\star)^{-1}$. Here H_\star is the Hubble rate at the time of instant source, and since source is during inflation, we have identified H_\star as the constant Hubble expansion rate during inflation. The GW metric, induced by the instant source, in the later period of inflation is expressed as

$$\begin{aligned} \tilde{h}_{ij}^{\text{Inf}}(\tau, \mathbf{k}) &= 16\pi G_N a_\star \tilde{\sigma}_{ij}(\mathbf{k}) \mathcal{G}_{\text{Inf}}(\tau - \tau_\star, \mathbf{k}) \\ &= 16\pi G_N \tilde{\sigma}_{ij}(\mathbf{k}) h_{\text{Inf}}(\tau, \mathbf{k}), \quad (\tau_i^{\text{Inf}} < \tau_\star < \tau < \tau_f^{\text{Inf}}) \end{aligned} \quad (2.17)$$

where τ_i^{Inf} and τ_f^{Inf} are initial and final values of the conformal time in the inflation era, respectively, and $h_{\text{Inf}}(\tau, \mathbf{k})$ is a scalar function defined as

$$h_{\text{Inf}}(\tau, \mathbf{k}) = \frac{a_\star}{k} \left[\frac{a_\star H_\star}{k} \left(\frac{a_\star}{a(\tau)} - 1 \right) \cos[k(\tau - \tau_\star)] + \left(\frac{a_\star^2 H_\star^2}{k^2} + \frac{a_\star}{a(\tau)} \right) \sin[k(\tau - \tau_\star)] \right]. \quad (2.18)$$

Then, we match the GW metric from the final time of inflation τ_f^{Inf} to the initial time of RD τ_i^{RD} . Using $t(\tau_f^{\text{Inf}}) = t(\tau_i^{\text{RD}}) = t_{\text{Rh}}$, the matching condition in Eq. (2.9) becomes

$$\begin{aligned} \tilde{h}_{ij}^{\text{Inf}}(\tau_f^{\text{Inf}}, \mathbf{k}) &= C_{ij,1}^{\text{RD}} h_1^{\text{RD}}(\tau_i^{\text{RD}}, \mathbf{k}) + C_{ij,2}^{\text{RD}} h_2^{\text{RD}}(\tau_i^{\text{RD}}, \mathbf{k}), \\ \partial_\tau \tilde{h}_{ij}^{\text{Inf}}(\tau, \mathbf{k}) \Big|_{\tau_f^{\text{Inf}}} &= C_{ij,1}^{\text{RD}} \partial_\tau \tilde{h}_1^{\text{RD}}(\tau, \mathbf{k}) \Big|_{\tau_i^{\text{RD}}} + C_{ij,2}^{\text{RD}} \partial_\tau \tilde{h}_2^{\text{RD}}(\tau, \mathbf{k}) \Big|_{\tau_i^{\text{RD}}}. \end{aligned} \quad (2.19)$$

$C_{ij,1}^{\text{RD}}$ and $C_{ij,2}^{\text{RD}}$ are solved to be

$$\begin{aligned} C_{ij,1}^{\text{RD}} &= 16\pi G_{\text{N}} \tilde{\sigma}_{ij}(\mathbf{k}) \frac{h_{\text{Inf}}(\frac{-1}{H_* a_{\text{Rh}}}, \mathbf{k}) \times (h_2^{\text{RD}})'(\frac{2t_{\text{Rh}}}{a_{\text{Rh}}}, \mathbf{k}) - h_{\text{Inf}}'(\frac{-1}{H_* a_{\text{Rh}}}, \mathbf{k}) \times h_2^{\text{RD}}(\frac{2t_{\text{Rh}}}{a_{\text{Rh}}}, \mathbf{k})}{h_1^{\text{RD}}(\frac{2t_{\text{Rh}}}{a_{\text{Rh}}}, \mathbf{k}) \times (h_2^{\text{RD}})'(\frac{2t_{\text{Rh}}}{a_{\text{Rh}}}, \mathbf{k}) - (h_1^{\text{RD}})'(\frac{2t_{\text{Rh}}}{a_{\text{Rh}}}, \mathbf{k}) \times h_2^{\text{RD}}(\frac{2t_{\text{Rh}}}{a_{\text{Rh}}}, \mathbf{k})}, \\ C_{ij,2}^{\text{RD}} &= 16\pi G_{\text{N}} \tilde{\sigma}_{ij}(\mathbf{k}) \frac{h_{\text{Inf}}(\frac{-1}{H_* a_{\text{Rh}}}, \mathbf{k}) \times (h_1^{\text{RD}})'(\frac{2t_{\text{Rh}}}{a_{\text{Rh}}}, \mathbf{k}) - h_{\text{Inf}}'(\frac{-1}{H_* a_{\text{Rh}}}, \mathbf{k}) \times h_1^{\text{RD}}(\frac{2t_{\text{Rh}}}{a_{\text{Rh}}}, \mathbf{k})}{h_2^{\text{RD}}(\frac{2t_{\text{Rh}}}{a_{\text{Rh}}}, \mathbf{k}) \times (h_1^{\text{RD}})'(\frac{2t_{\text{Rh}}}{a_{\text{Rh}}}, \mathbf{k}) - (h_2^{\text{RD}})'(\frac{2t_{\text{Rh}}}{a_{\text{Rh}}}, \mathbf{k}) \times h_1^{\text{RD}}(\frac{2t_{\text{Rh}}}{a_{\text{Rh}}}, \mathbf{k})}. \end{aligned} \quad (2.20)$$

Therefore, the GW metric during RD period is converted to

$$\tilde{h}_{ij}^{\text{RD}}(\tau, \mathbf{k}) = 16\pi G_{\text{N}} \tilde{\sigma}_{ij}(\mathbf{k}) \times h_{\text{RD}}(\tau, \mathbf{k}), \quad (\tau_1^{\text{RD}} < \tau) \quad (2.21)$$

where $h_{\text{RD}}(\tau, \mathbf{k})$ is a scale function defined as

$$\begin{aligned} h_{\text{RD}}(\tau, \mathbf{k}) &= h_0(\tau, \mathbf{k}) + h_1(\tau, \mathbf{k}), \\ h_0(\tau, \mathbf{k}) &= \frac{-a_{\text{Rh}}^2}{a(\tau)} \frac{1}{a_* H_*} \left\{ \cos[y(1-\epsilon)] - \frac{\sin[y(1-\epsilon)]}{y} \right\} \frac{\sin[k\tau - y\epsilon]}{y^3}, \\ h_1(\tau, \mathbf{k}) &= \frac{-a_{\text{Rh}}^2}{a(\tau)} \frac{y\epsilon}{a_* H_*} \left\{ \frac{1-\epsilon}{y^3} \cos[k\tau + y(1-2\epsilon)] - \left(\frac{1+y\epsilon}{y^4} \right) \sin[k\tau + y(1-2\epsilon)] \right\} \end{aligned} \quad (2.22)$$

with

$$y = \frac{k}{a_* H_*}, \quad \epsilon = \frac{a_*}{a_{\text{Rh}}}. \quad (2.23)$$

Here we have specified h_{RD} into two terms. The first term $h_0(\tau, \mathbf{k})$ dominates $h_{\text{RD}}(\tau, \mathbf{k})$ for $y\epsilon \ll 1$, and the second term $h_1(\tau, \mathbf{k})$ dominates $h_{\text{RD}}(\tau, \mathbf{k})$ for $y\epsilon \gg 1$.

The GW energy density is obtained from the derivative

$$\partial_\tau \tilde{h}_{ij}^{\text{RD}}(\tau, \mathbf{k}) = 16\pi G_{\text{N}} \tilde{\sigma}_{ij}(\mathbf{k}) \times \partial_\tau h_{\text{RD}}(\tau, \mathbf{k}). \quad (2.24)$$

From the above, it is straightforward to obtain the GW energy density per log k as

$$\frac{d\rho_{\text{GW}}}{d \log k} = \frac{d\rho_{\text{GW}}^{\text{flat}}}{d \log k} \times \frac{a_{\text{Rh}}^4}{a^4(t)} \times \mathcal{S}(t, k), \quad (t_{\text{f}}^{\text{Inf}} < t \leq t_0) \quad (2.25)$$

where

$$\frac{d\rho_{\text{GW}}^{\text{flat}}}{d \log k} = \frac{2G_{\text{N}}}{\pi} \frac{k^3}{V} |\tilde{\sigma}_{ij}(\mathbf{k})|^2 \quad (2.26)$$

is the GW energy density per log k just in flat spacetime,² and

$$\begin{aligned} \mathcal{S}(t, k) &= \left(1 + \frac{a_{\text{Rh}}^4}{a^2(t) a_*^2 y^2} \right) \left\{ \left[\frac{\cos[y(1-\epsilon)]}{y^2} - \frac{\sin[y(1-\epsilon)]}{y^3} \right]^2 \right. \\ &\quad \left. + \epsilon \left[\frac{1}{y^2} + 2 - \epsilon \right] \frac{\sin[2y(1-\epsilon)]}{y^3} - \epsilon \left[\frac{2-\epsilon}{y^2} + \epsilon \right] \frac{\cos[2y(1-\epsilon)]}{y^2} + \epsilon^4 \left(\frac{1}{y^2} + 1 \right) \right\}, \end{aligned} \quad (2.27)$$

²This is obtained by setting $\mathcal{H} = 0$ in Eq. (2.6). Then the metric is solved to be $h_{ij}^{\text{flat}}(\tau, \mathbf{k}) = 16\pi G_{\text{N}} \tilde{\sigma}_{ij}(\mathbf{k}) \sin[k(\tau - \tau_*)]/k$, and Eq.(2.26) is obtained just following the definition in Eq. (2.13). The superscript ‘‘flat’’ represents the GW spectrum obtained in the flat spacetime.

is a momentum-dependent deformation function modifying the shape of the GW spectrum via inflation. The second term $\frac{a_{\text{Rh}}^4}{a^2(t)a_*^2y^2}$ in the parentheses arises from the derivative of the co-moving factor $a(t)$ of Eq (2.22). By fixing the time at today ($a(t_0) = a_0$), $\frac{a_{\text{Rh}}^2}{a_0a_*y} \ll 1$ is in general satisfied for frequency $f \geq 10^{-18}$ Hz. In the above expression, the oscillation in the metric (via the $\sin(k\tau)$ and $\cos(k\tau)$ terms) has been averaged following the integration $\int_{T_r} d\tau$. On the other hand, as EOMs of GWs in different era are different, matching from the end of previous period to the beginning of next period, mainly the end of inflation to the beginning of RD, leads to oscillation in the energy spectrum of GW background.

The next is to consider the matching from RD to MD, and that from MD to Λ D eras. For GW frequency of our interests, i.e. $f \gtrsim 10^{-9}$ Hz, as the GWs are always inside the horizon during RD, MD and Λ D, the matching is trivial and we dismiss it in this study. On the other hand, for lower frequency, in particular, for $f \leq 10^{-14}$ Hz, the matching at the matter-radiation equality should be considered.

We further compare the presently inflated GW spectrum $\Omega_{\text{GW}}(f)$ with the uninflated spectrum $\tilde{\Omega}_{\text{GW}}(\tilde{f})$. The latter, more precisely, is the GW spectrum generated from the same instant source, in the radiation era after the reheating. We fix source in the beginning of the RD era, just after the reheating. The hypothetical frequency not redshifted by inflation, \tilde{f} , correlates with the physical frequency f via $\tilde{f} = f a_{\text{Rh}}/a_*$. The correlation between inflated and uninflated GW spectrums is straightforwardly obtained as

$$h^2\Omega_{\text{GW}}(f) = h^2\tilde{\Omega}_{\text{GW}}(\tilde{f}) \Big|_{\tilde{f}=f\frac{a_{\text{Rh}}}{a_*}} \times S(f). \quad (2.28)$$

Here,

$$h^2\tilde{\Omega}_{\text{GW}}(\tilde{f}) = \frac{h^2}{\rho_c} \frac{d\rho_{\text{GW}}^{\text{flat}}}{d \log k} \times \frac{a_{\text{Rh}}^4}{a_0^4} \quad (2.29)$$

is the uninflated GW spectrum which is supposed to be observed today. As we assumed instant source happens in the beginning of the radiation era, thus the scale factor have been replaced by a_{Rh} . $S(f)$ is the momentum-dependent deformation function with time set at today, $S(f) \equiv \mathcal{S}(t_0, k=2\pi a_0 f)$. We further divided it into two terms

$$S(f) = S_0(f) + S_1(f) \quad (2.30)$$

with

$$S_0(f) = \left\{ \frac{\cos[y(1-\epsilon)]}{y^2} - \frac{\sin[y(1-\epsilon)]}{y^3} \right\}^2 \Big|_{y=\frac{2\pi a_0 f}{a_* H_*}}, \quad (2.31)$$

$$S_1(f) = y\epsilon \times \left\{ \left[\frac{1}{y^2} + 2 - \epsilon \right] \frac{\sin[2y(1-\epsilon)]}{y^4} - \left[\frac{2-\epsilon}{y^2} + \epsilon \right] \frac{\cos[2y(1-\epsilon)]}{y^3} + \frac{\epsilon^3}{y} \left(\frac{1}{y^2} + 1 \right) \right\} \Big|_{y=\frac{2\pi a_0 f}{a_* H_*}}. \quad (2.32)$$

$S_0(f)$ is the leading contribution for $y\epsilon \ll 1$, which is directly derived via $h_0(\tau, \mathbf{k})$ in Eq. (2.22). This is exactly the result listed in [25]. $S_1(f)$ includes the rest terms. In the

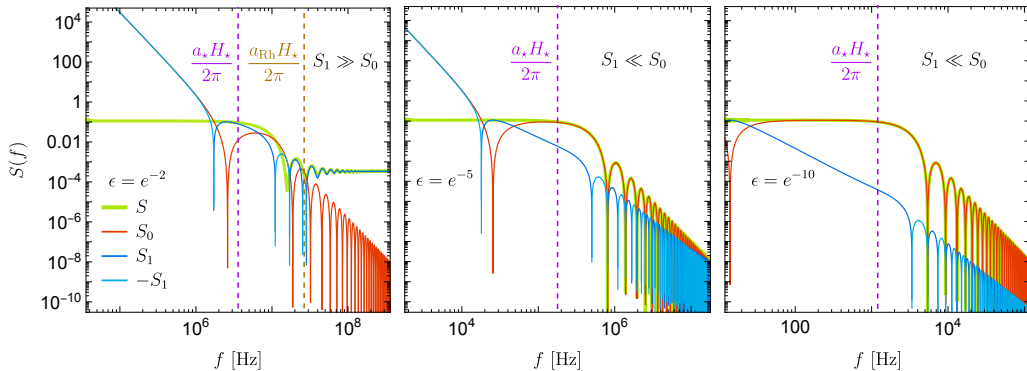


Figure 1. Deformation function along the frequency with inputs $T_{\text{Rh}} = 10^{15}$ GeV, $\epsilon = e^{-2}$ (left), e^{-5} (middle) and e^{-10} (right).

high frequency band $y\epsilon \gg 1$, $S_1(f)$ can be dominant and thus, we keep it in our formula. We show in Fig. 1 the comparison of $S_0(f)$ and $S_1(f)$ along the frequency. More discussions are given in the next subsection.

2.3 IR and UV behaviour of the inflated GW spectrum

We discuss in more details on IR and UV behaviours of GW spectrum obtained in the last subsection. The IR and UV bands of the inflated GW spectrum are distinguished by comparing the physical GW wavelength $\lambda_\star = 2\pi a_\star/k$ at the time of GW produced with the Hubble distance H_\star^{-1} . $\lambda_\star \gg H_\star^{-1}$ refers to the IR band and on the contrary is the UV band. In addition, we specify the Far UV (FUV) band if the physical wavelength at the end of the inflation, which has been redshifted by a factor a_{Rh}/a_\star , is much shorter than the Hubble distance at that time, i.e., $\lambda_\star a_{\text{Rh}}/a_\star \ll H_\star^{-1}$. The three regimes expressed in frequency today are respectively given by

$$\begin{aligned}
 \text{IR :} \quad k &\ll a_\star H_\star &\Rightarrow & f \ll \frac{a_\star H_\star}{2\pi a_0}, \\
 \text{UV :} \quad a_\star H_\star &\ll k \ll a_{\text{Rh}} H_\star &\Rightarrow & \frac{a_\star H_\star}{2\pi a_0} \ll f \ll \frac{a_{\text{Rh}} H_\star}{2\pi a_0}, \\
 \text{FUV :} \quad k &\gg a_{\text{Rh}} H_\star &\Rightarrow & f \gg \frac{a_{\text{Rh}} H_\star}{2\pi a_0}.
 \end{aligned} \tag{2.33}$$

These regimes are also indicated in Fig. 1. On the other hand, since the parameter $y = \frac{2\pi a_0 f}{a_\star H_\star}$ in oscillation terms of the deformation function takes a key role to determine the shape of the spectrum, we can also distinguish the IR, UV, and FUV bands via conditions $y \ll 1$, $1 \ll y \ll 1/\epsilon$ and $y \gg 1/\epsilon$, respectively.

Given the formulation in the last subsection, we outline the IR, UV and FUV behaviour of the inflated GW spectrum below.

- In the IR band, the wavelength of GWs is outside the horizon during the whole period of inflation and moves back to the horizon after reheating. Therefore, the metric of

GWs in the IR band is hardly diluted by inflation, $\tilde{h}_{ij}^{\text{RD}}(\tau, \mathbf{k})|_{y \ll 1} \propto \frac{a_{\text{Rh}}^2}{a(t)}$, and from (2.22), we can get

$$h_{\text{RD}}^{\text{IR}} \simeq \frac{1}{k} \frac{a_{\text{Rh}}^2}{a(t)} \times \frac{1}{3} \sin\left(k\tau - \frac{k}{a_{\text{Rh}} H_\star}\right). \quad (2.34)$$

The deformation function of the GW spectrum in the IR band approximates to

$$S(f)^{\text{IR}} \simeq \frac{1}{9}. \quad (2.35)$$

The energy density of this case is not strongly diluted and is almost the same as it without inflation except the suppression factor $1/9$. In the above approximation, we have assumed $\epsilon \ll 1$ which is in general true during the inflation. If it does not hold, the factors $1/3$ in Eq. (2.34) and $1/9$ in Eq. (2.35) should be replaced by $(1 + 2\epsilon^2)/3$ and $(1 + 2\epsilon^2)^2/9$, respectively.

- In the UV but not the FUV band, the wavelength is inside the horizon during the GW production, and then get redshifted outside the horizon before the end of the inflation. It moves back to the horizon at later time after the inflation. The GW metric approximates to

$$h_{\text{RD}}^{\text{UV}} \simeq \frac{-1}{k} \frac{a_{\text{Rh}}^2}{a(\tau)} \frac{\cos[y(1 - \epsilon)]}{y^2} \sin(k\tau - y\epsilon). \quad (2.36)$$

Again we have assumed $\epsilon \ll 1$. The spectrum deformation function approximates to

$$S(f)^{\text{UV}} \simeq \frac{\cos[2y(1 - \epsilon)] + 1}{2y^4}. \quad (2.37)$$

As we have not moved to the FUV regime, $y\epsilon < 1$, $S_0(f)$ still dominates the deformation function $S(f)$. Thus, the oscillation behaviour is important in this regime.

- In the FUV band, the wavelength of GWs is always inside the horizon. Hence, the GW metric gives

$$h_{\text{RD}}^{\text{FUV}} \simeq \frac{1}{k} \frac{a_\star^2}{a(t)} \sin[k\tau + y(1 - 2\epsilon)]. \quad (2.38)$$

The deformation function provides only a suppression factor,

$$S^{\text{FUV}}(f) \simeq \frac{a_\star^4}{a_{\text{Rh}}^4}. \quad (2.39)$$

Due to the quartic dependence, a small fraction a_\star/a_{Rh} leads to a large suppression to the FUV regime. Once the GW happens significantly before the end of the inflation, the GWs in the FUV band will be highly diluted and thus is almost not observable.

Note the discussion in the above depends only on the instant-source approximation. On the other hand, if the instant-source assumption works in a realistic dynamics, these discussions apply, in spite of the explicit form of GW source. In the coming section, we will focus on GUT phase transition and show more features of the spectrum of its inflated GWs.

3 Application to GUT phase transition

GUTs provide a strong motivation to study phase transition (PT) during the inflation. The monopole problem in GUTs is one important reason to propose an inflationary period before the radiation era. To dilute the energy density of GUT monopoles, the GUT symmetry breaking should take place before or during inflation. Here we will specify the GUT PT is instantaneous and happens at some point during the inflation, and it is triggered by the varying inflaton field at a certain number of e-folds during the inflation. We denote

$$N_\star = \log \frac{a_{\text{Rh}}}{a_\star} \quad (3.1)$$

as the e-folding number of PT. In a certain regime of N_\star , we will see that the GW frequency induced by the GUT PT can be redshifted into the observable regime in the foreseeable future and the cosmological monopole problem is solved.

3.1 Solution to the monopole problem

We first give briefly review on how the monopole problem triggered GUT PT is solved by an inflation. It is well-known that a GUT symmetry breaking in the very early Universe, either $SU(5)$ GUT or $SO(10)$ GUT, leads to the generation of monopoles with mass M_{mono} at the GUT scale. Given an initial number density of monopoles at their production $n_\star = n_{\text{mono}}(t_\star)$, the evolution of monopoles is like the matter, with its number density at later time following

$$n_{\text{mono}}(t) = \left(\frac{a(t_\star)}{a(t)} \right)^3 n_\star. \quad (3.2)$$

The energy density fraction of monopoles today is given by $\Omega_{\text{mono}} = M_{\text{mono}} n_{\text{mono}}(t_0) / \rho_c$ with $\rho_c = 3H_0^2 / (8\pi G_{\text{N}})$ the critical energy density today. The initial number density is given by the initial correlation length $n_\star = L_{\text{mono},\star}^{-3}$, where $L_{\text{mono},\star}$ is at the same order of the Hubble distance, and here we take $L_{\text{mono},\star} \simeq H_\star^{-1}$ for simplicity. It is well-known that the GUT monopoles cannot be produced in the radiation era. Namely, by taking the monopole mass and the thermal temperature at the GUT scale, we arrive at $\Omega_{\text{mono}} \gg 10^{-6}$ which conflicts with the observed Universe.

Therefore, we consider the PT happening during inflation. Monopoles, which are generated just following the completion of PT, have the initial correlation length of the same order of the Hubble distance at inflation. Again, we assume $L_{\text{mono},\star} = H_\star^{-1}$ for simplicity. Given the e-folding number N_\star in Eq. (3.1), we obtain Ω_{mono} is diluted to

$$\Omega_{\text{mono}} = \frac{8\pi G M_{\text{mono}} H_\star^3}{3H_0^2 (1 + z_{\text{Rh}})^3} e^{-3N_\star}. \quad (3.3)$$

We make naive approximations $H_\star \sim H_{\text{Rh}} \simeq 0.1 T_{\text{Rh}}^2 / M_{\text{pl}}$ and $M_{\text{mono}} \sim T_{\text{Rh}}$, and arrive at

$$\Omega_{\text{mono}} \sim 10^{-6} \left(\frac{T_{\text{Rh}}}{10^{15} \text{ GeV}} \right)^4 e^{-3(N_\star - 15)}. \quad (3.4)$$

Taking the GUT monopole mass $T_{\text{Rh}} \sim 10^{15}$ GeV, we should restrict the e-folding number at the PT $N_\star \gtrsim 15$, such that $\Omega_{\text{mono}} \lesssim 10^{-6}$ is small enough to satisfy the cosmological constraints. Note that Eq. (3.4) applies also to monopole generated from intermediate symmetry breaking below the GUT scale but sufficiently higher than the electroweak scale. For example, we take the Pati-Salam scale at 10^{14} GeV and assume the relevant monopole mass and reheating temperature around the same scale, the requirement $\Omega_{\text{mono}} \lesssim 10^{-6}$ relaxes the restriction on the number of e-folds to $N_\star \gtrsim 12$.

3.2 Inflated GWs via GUT phase transition

A first-order GUT PT can happen in the inflationary era. Different from the widely studied thermal PT in the radiation era, where the temperature plays the crucial role. The slow-roll inflation field may take the role in the PT during inflation.

Whether a first-order PT can occur depends on the form of the effective potential during the PT. Without knowing the detail of GUT, we do not know the explicit form of the effective potential during the PT. Although our latter discussion does not depend on any details of the form of the potential for instant PT, we show one typical example which might point to a large class of GUT models. We denote the higgs field which breaks the GUT gauge symmetry as σ , and the inflaton field ϕ is considered a slow-roll background field. As an analogy, the potential terms relevant for GUT PT take the form,

$$V_{\text{PT}}(\phi, \sigma) = D(\phi^2 - \phi_0^2)\sigma^2 - \mu\sigma^3 + \frac{\lambda}{4}\sigma^4, \quad (3.5)$$

where ϕ_0 is a constant, and μ and λ are either constants or ϕ -insensitive functions. Here we have not written out the potential for ϕ which dominates the inflation and also ignored the influence of σ on the evolution of inflation. During the inflation, the inflaton field ϕ , as a background, gradually diminishes from a value sufficiently larger than ϕ_0 . The potential along the σ direction is minimised at $\sigma = 0$. Until ϕ drops to the critical value $\phi_c \equiv \sqrt{\phi_0^2 + \frac{\mu^2}{\lambda D}}$, two vacua $\sigma = 0, v_\sigma$ (where $v_\sigma = \frac{3\mu}{2\lambda} + [\frac{9\mu^2}{4\lambda^2} - \frac{2D}{\lambda}(\phi^2 - \phi_0^2)]^{1/2}$) become degenerate. The PT of σ from 0 to v_σ should happen at some point for ϕ varying from ϕ_c to ϕ_0 .

Gravitational waves are generated during the PT when the energy from the false vacuum to the bulk. The shape of the GW spectrum depends on gravitational emission modes. In most studies of PTs in the radiation era, three modes are widely considered: direct release during bubble wall collisions, sound waves in the plasma after bubble wall collisions, and turbulence in the plasma after the collisions, seeing [30] for a review. Here the first mode is more relevant in our particular study.

We apply the envelope approximation [31–34] to formulate the GW spectrum in the bubble wall collision modes. In this approximation, a fraction κ of the latent heat of the PT is deposited in a thin shell close to the PT front. The energy in each shell is assumed to quickly disperse after colliding with another shell such that the energy is primarily stored in the envelope of uncollided shells. Numerical simulations in the envelope approximation suggest that the GW spectrum at the moment just after PT follows a broken power law

[35]. Here we briefly summarised the formula below.

$$\Omega_{\text{GW}\star}(f_\star) \equiv \frac{1}{\rho_{\text{tot}}} \frac{d\rho_{\text{GW}}^{\text{flat}}}{d \log f_\star} = \Omega_{\text{GW}\star}^{\text{peak}} \frac{(a+b)(f_\star/f_\star^{\text{peak}})^a}{a(f_\star/f_\star^{\text{peak}})^{a+b} + b}. \quad (3.6)$$

The spectral indices $a = 2.8$ and $b = 1$ are suggested, providing a better fit to the simulation result not too far away from the peak, in spite that causality implies $a = 3$ [36, 37]. The peak amplitude and peak frequency are respectively given by

$$\Omega_{\text{GW}\star}^{\text{peak}} = \frac{0.11 v_w^3}{0.42 + v_w^2} \times \kappa^2 \left(\frac{H_\star}{\beta} \right)^2 \left(\frac{\rho_{\text{PT}}}{\rho_{\text{tot}}} \right)^2, \quad (3.7)$$

$$f_\star^{\text{peak}} = \frac{0.62 \beta}{1.8 - 0.1 v_w + v_w^2}, \quad (3.8)$$

where $H_\star^2 = \frac{8}{3} \pi G_{\text{N}} \rho_{\text{tot}}$ has been used. The peak amplitude is proportional to the square of $\rho_{\text{PT}}/\rho_{\text{tot}}$. ρ_{PT} is the difference of energy density between the true and the false vacua. β^{-1} represents the duration of the PT. v_w is the bubble wall velocity which will be approximated at $v_w \approx 1$ in this work. κ is the efficiency factor for vacuum energy transformed into kinetic energy of the bulk fluid. Given the ratio of the vacua energy difference to the radiation energy $\alpha = \rho_{\text{PT}}/\rho_{\text{rad}}$, the efficiency factor is calculated to be

$$\kappa(\alpha) = \frac{0.715\alpha + 0.181\sqrt{\alpha}}{1 + 0.715\alpha}. \quad (3.9)$$

This factor approaches to 1 in the limit $\alpha \rightarrow \infty$. In the radiation era where $\rho_{\text{tot}} = \rho_{\text{PT}} + \rho_{\text{rad}}$, the peak amplitude is re-written to be

$$\Omega_{\text{GW}\star}^{\text{peak}} = \frac{0.11 v_w^3}{0.42 + v_w^2} \times \kappa^2 \left(\frac{H_\star}{\beta} \right)^2 \left(\frac{\alpha}{\alpha + 1} \right)^2, \quad (3.10)$$

where is exactly the formula appearing in [35]. However, we keep in mind that there might be additional energy budgets present during the PT. This is exactly what we will discuss soon in the PT during the inflationary era, where the total energy should be $\rho_{\text{tot}} = \rho_{\text{Inf}} + \rho_{\text{PT}} + \rho_{\text{rad}}$ and ρ_{Inf} dominates the total energy.

In our particular case, by assuming $v_w \approx 1$ and setting the limit $\alpha \rightarrow \infty$, we convert the spectrum $\Omega_{\text{GW}\star}(f_\star)$ to the redshifted one,

$$\begin{aligned} h^2 \tilde{\Omega}_{\text{GW}}(\tilde{f}) &= 1.27 \times 10^{-6} \times \left(\frac{H_\star}{\beta} \right)^2 \left(\frac{\rho_{\text{PT}}}{\rho_{\text{tot}}} \right)^2 \left(\frac{100}{g_\star} \right)^{1/3} \times \frac{(a+b)(\tilde{f}/\tilde{f}^{\text{peak}})^a}{a(\tilde{f}/\tilde{f}^{\text{peak}})^{a+b} + b}, \\ \tilde{f}^{\text{peak}} &= 37.8 \text{ MHz} \times \left(\frac{\beta}{H_\star} \right) \left(\frac{T_\star}{10^{15} \text{ GeV}} \right) \left(\frac{g_\star}{100} \right)^{1/6}, \end{aligned} \quad (3.11)$$

where $f_\star^{\text{peak}}/\beta \approx 0.23$ at $v_w \approx 1$ has been used.

Considering the PT as an instant source at N_\star during the inflation, we include the deformation function $S(f)$ to the above spectrum, and obtain the inflated GW spectrum $h^2 \Omega_{\text{GW}}(f)$

$$h^2 \Omega_{\text{GW}}(f) = h^2 \tilde{\Omega}_{\text{GW}}(f e^{N_\star}) \times S(f) \quad (3.12)$$

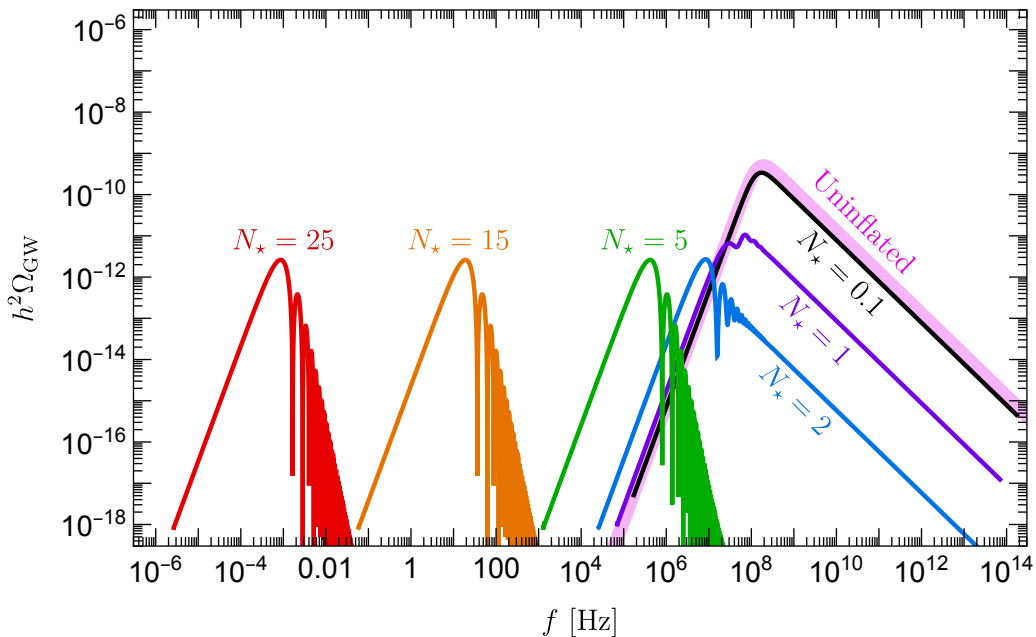


Figure 2. Comparison of GW spectra with or without modification by inflation. Inflated GW spectra for the e-folding number $N_\star = 0.1, 1, 2, 5, 15, 25$ are presented. The uninflated GW spectrum is obtained in the envelope approximation with the phase transition temperature assumed to be $T_\star = T_{\text{Rh}}$. Input parameters: $T_{\text{Rh}} = 10^{15}$ GeV, $\rho_{\text{PT}}/\rho_{\text{tot}} = 0.1$, $\beta/H_\star = 5$.

following Eq. (2.28) with the temperature T_\star replaced by the reheating temperature T_{Rh} . Here g_\star should be understood as the degree of freedom of radiation in the beginning of the RD era. As a comparison, $h^2\tilde{\Omega}_{\text{GW}}(\tilde{f})$, with $\tilde{f} = fe^{N_\star}$, is the corresponding GW spectrum not modified by inflation. We show in Fig. 2 the inflated GW spectra with the e-folding number $N_\star = 0.1, 1, 2, 5, 15, 25$, respectively. The uninflated spectrum, i.e., GWs produced after reheating, is shown as a comparison. For $N_\star \rightarrow 0$, inflated GW spectrum can go back to the spectrum without inflation. As shown, the strength of GWs is suppressed, and its shape is deformed and frequency is redshifted with N_\star increasing from 0 to 5. At $N_\star = 2$, the shape of the spectrum shows clearly distinguishable behaviours in the IR, UV and FUV bands. For $N_\star \gtrsim 5$, the GW spectrum in the FUV band is highly suppressed and not shown in the plot. For N varying from 5 to large values, the strength and shape of GW spectrum keep insensitive to the value of N_\star , and only the frequency get redshift following the e-folding number N_\star . The uninflated GWs with peak frequency around 0.1 GHz is shifted to 10 Hz and mHz for $N_\star \simeq 15$ and 25, respectively.

It is worth mentioning that the peak of the inflated spectrum is not simply a redshift from the peak of the uninflated spectrum. First of all, the peak frequency f^{peak} is almost irrelevant to \tilde{f}^{peak} . While the latter, the uninflated peak frequency \tilde{f}^{peak} , is proportional to the inverse duration of PT β/H_\star , the inflated peak frequency f^{peak} is determined by the first peak of the oscillation term in the deformation function $\mathcal{S}(f)$. For $\beta/H_\star > 5$, where

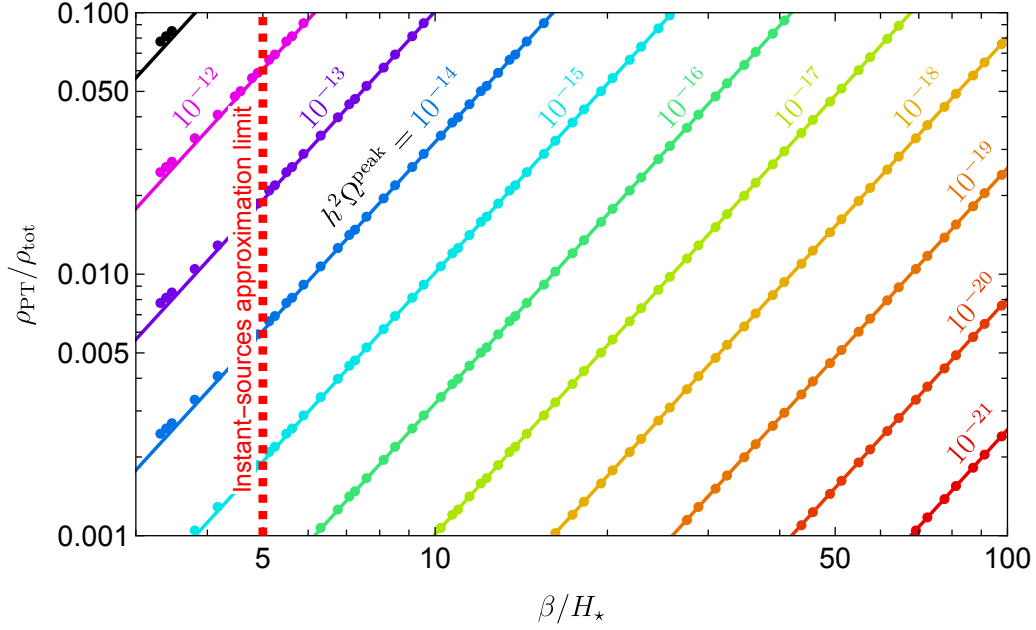


Figure 3. This figure is that different peak value of GW spectrum $h^2\Omega_{\text{GW}}^{\text{peak}}$ is decided by PT velocity β/H_* and PT energy proportion $\rho_{\text{PT}}/\rho_{\text{tot}}$. Input parameters: $T_{\text{Rh}} = 10^{15}$ GeV, $N_* = 36$ and $v_w = 1$. The points are numerical solutions from Eq. (3.12), and the solid lines are approximately analytic by Eq. (3.15). The region $\beta/H_* \geq 5$ to apply the instant-source approximation is indicated.

the instant-source approximation applies, the near peak GW spectrum satisfies

$$h^2\Omega_{\text{GW}}(f) \propto f^a S_0(f). \quad (3.13)$$

By extremising the RHS of the above formula, we derive $y^{\text{peak}} = 2.394$ and $S_0(f^{\text{peak}}) = 0.0315$ for $a = 2.8$. The peak frequency is straightforwardly obtained as

$$f^{\text{peak}} \simeq 62.7 \text{ MHz} \times \left(\frac{g_*}{100}\right)^{1/6} \left(\frac{T_*}{10^{15} \text{ GeV}}\right) \times e^{-N_*}, \quad (3.14)$$

which is insensitive to the value of β/H_* . The peak amplitude at this point approximates to

$$\begin{aligned} h^2\Omega_{\text{GW}}^{\text{peak}} &\approx S_0(f^{\text{peak}}) \times h^2\tilde{\Omega}_{\text{GW}}(f^{\text{peak}} e^{N_*}) \\ &\approx 6.27 \times 10^{-7} \times \left(\frac{H_*}{\beta}\right)^{2+a} \left(\frac{\rho_{\text{PT}}}{\rho_{\text{tot}}}\right)^2 \left(\frac{100}{g_*}\right)^{1/3}. \end{aligned} \quad (3.15)$$

In Fig. 3, we show that the analytical approximation matches very well with the numerical calculation. The main point from the analytical formula is the prove of the highly dependence of the peak amplitude on the inverse duration of PT, $\Omega_{\text{GW}}^{\text{peak}} \propto (\beta/H)^{-2-a} \sim (\beta/H)^{-5}$ and the independence of N_* (for $N_* > 5$). In order to generate an observable GW signal (e.g., by requiring $\Omega_{\text{GW}}^{\text{peak}} > 10^{-16}$), $\beta/H_* \gtrsim 50$ should be roughly required, depending on the fraction $\rho_{\text{PT}}/\rho_{\text{tot}}$.

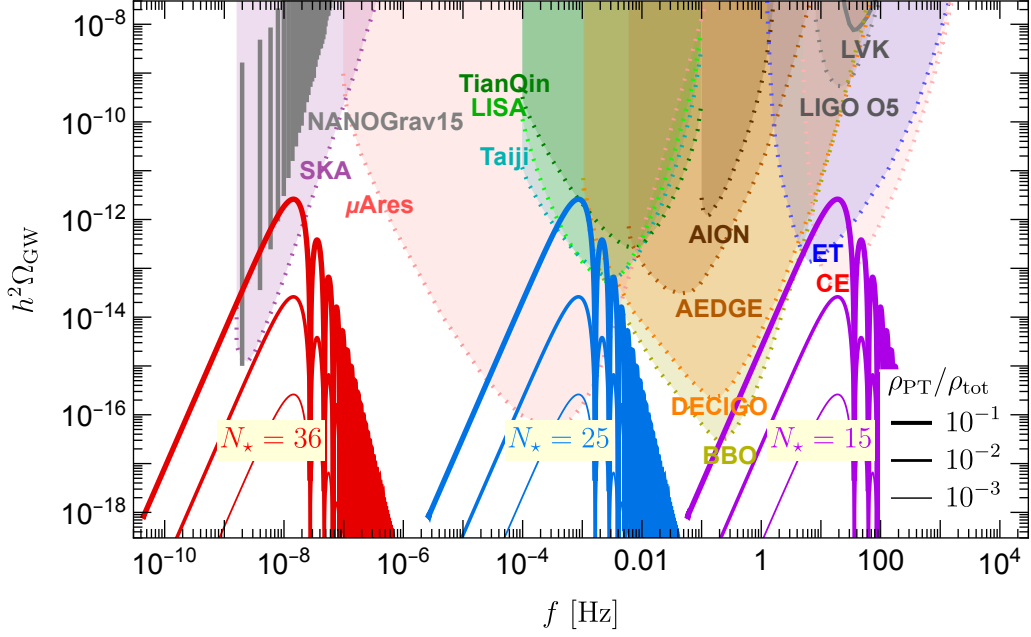


Figure 4. Inflated spectrum of GWs from GUT phase transition on different e-folding number of time of GW production $N_* = 15, 25$ and 36 (violet, blue, red, respectively) and different PT energy proportion $\rho_{\text{PT}}/\rho_{\text{tot}} = 0.1, 0.01$ and 0.001 (curve thickness of thick, middle and thin, respectively). $\beta/H_* = 5$, $T_{\text{Rh}} = 10^{15}$ GeV and $v_w = 1$ are taken.

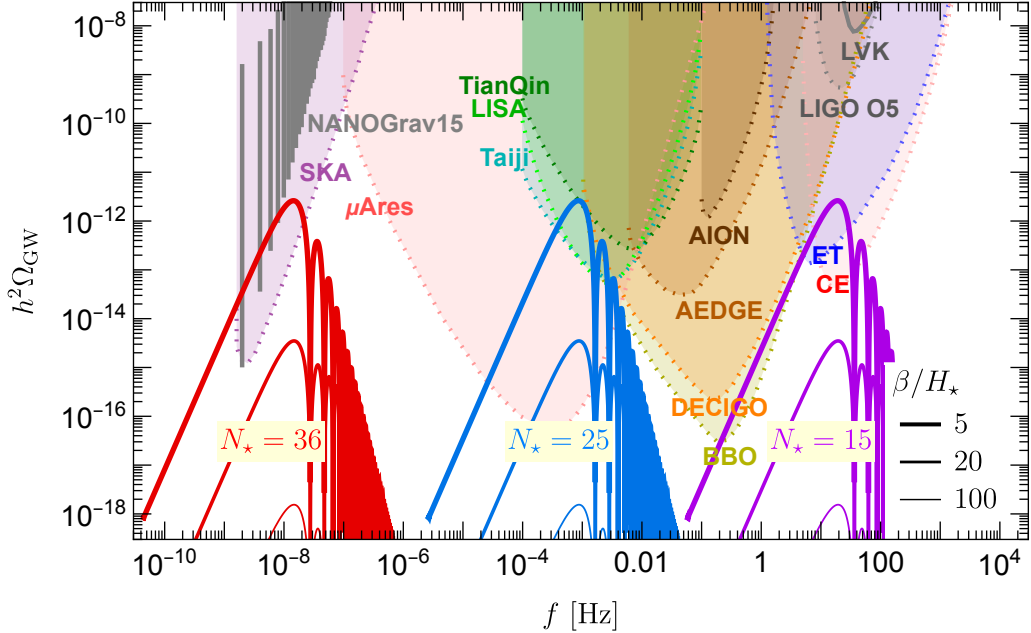


Figure 5. Inflated spectrum of GWs from GUT phase transition on different e-folds number of time of GW production $N_* = 15, 25$ and 36 (violet, blue, red, respectively) and inverse duration of PT $\beta/H_* = 5, 20$ and 100 (curve thickness of thick, middle and thin, respectively). $\rho_{\text{PT}}/\rho_{\text{tot}} = 0.1$, $T_{\text{Rh}} = 10^{15}$ GeV and $v_w = 1$ are taken.

We further show the inflated spectrum by varying the energy fraction $\rho_{\text{PT}}/\rho_{\text{Inf}}$ and the inverse duration of PT β/H in Fig. 4 and 5, respectively. For references, power-law integrated sensitivities for upcoming GW observatories, including space-based laser interferometers (LISA [38], Taiji [39], TianQin [40], BBO [41], DECIGO [42], μAres [43]), atomic interferometers (MAGIS [44], AEDGE [45], AION [46]), and ground-based interferometers (ET [47], CE [48]), and Square Kilometre Array [49] (SKA) are shown. $N_\star \simeq 15$ and 25 push the peak frequency to 10 Hz and 1 mHz, respectively. Those are perfect regimes to be tested in ground-based and space-based laser interferometers. The space-based experiments LISA and Taiji will be able to touch the the peak amplitude 10^{-13} at the best, corresponding to $\rho_{\text{PT}}/\rho_{\text{tot}} > 0.02$ for $\beta/H_\star = 5$ or $\rho_{\text{PT}}/\rho_{\text{tot}} > 0.1$ for $\beta/H_\star = 10$, seen in Fig. 3. The best sensitivity of GW measurements in the foreseeable future may touch 10^{-16} , referring to $\rho_{\text{PT}}/\rho_{\text{tot}} \approx 5 \times 10^{-4}$ at $\beta/H_\star = 5$ and $\rho_{\text{PT}}/\rho_{\text{tot}} \approx 0.1$ at $\beta/H_\star = 40$. The targeted region based on the NANOGrav 15 data [50] and the LIGO/Virgo/KAGRA (LVK) bound [51] set are also presented briefly in the figures. A large e-folding number $N_\star \sim 35$ can shift the frequency to the nHz regime. However, due to the highly suppression of $(\beta/H_\star)^{-2-a}$ and $(\rho_{\text{PT}}/\rho_{\text{tot}})^2$, a sufficiently strong signal $h^2\Omega_{\text{GW}}^{\text{peak}} \sim 10^{-9}$ is hard to reach for inflated GW via GUT PT in the instant-source approximation. However, another mechanism of GW production, i.e., the so-called secondary GWs from curvature perturbation induced by the phase transition during inflation, might provide a signal to matching with the PTA hint [27].

3.3 Inflated GWs via phase transition below GUT scale

Below the GUT scale, there might be some gauge symmetries persist at some intermediate scales from the GUT breaking to the SM. Some widely studied symmetries, e.g., the Pati-Salam symmetry $SU(4)_c \times SU(2)_L \times SU(2)_R$ via the breaking of $SO(10)$, the 333 model $SU(3)_c \times SU(3)_L \times SU(3)_R$ via the breaking of E_6 . Their energy scales are naturally assumed to be at a very high scale but not sufficiently as high as the GUT scale. Here we will focus on the scale between 10^{10} - 10^{15} GeV. On the other hand, the breaking of these symmetries generate monopoles with masses around the same scale of the symmetry breaking [52, 53]. Monopoles might still a problem if they are heavy enough, and the inflation should be introduced to solve the problem. Below we generalise the discussion in section 3.2 to inflated GWs via PT below the GUT scale. We relax the reheating temperature T_{Rh} in the range 10^{10} - 10^{15} GeV. The PT for intermediate symmetry breaking is assumed during the inflation with e-folding number N_\star of GUT PT. The monopole mass is again assumed at the same scale of T_{Rh} .

Relaxing the reheating temperature to a lower scale, the inflated GW spectrum formula in Eq. (3.12) still works. We apply it and show the dependence of the spectrum on the reheating temperature in Fig. 3.3. It is obvious that T_{Rh} only affects the redshift of frequency and does not change the amplitude and shape of the GW spectrum. We finally show the dependence of the peak frequency on the reheating temperature as well as the e-folding number N_\star in Fig. 7. Both numerical result (dots) based on Eq. (3.12) and analytical result (lines) in Eq. (3.14) are shown for comparison.

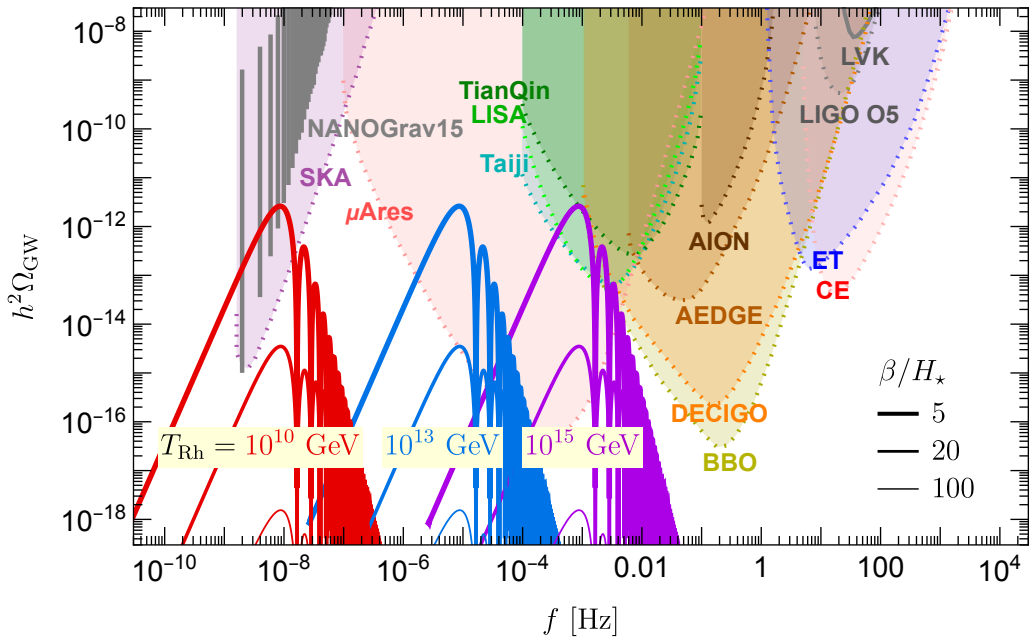


Figure 6. Inflated spectrum of GWs from phase transition at different reheating temperature $T_{\text{Rh}} = 10^{15}$, 10^{13} and 10^{10} GeV (shown in violet, blue and red, respectively) and the inverse duration of PT β/H_* = 5, 20 and 100 (thick, middle, thin, respectively). $N_* = 25$, $\rho_{\text{PT}}/\rho_{\text{tot}} = 0.1$, $v_w = 1$ are taken as inputs.

4 Conclusions

Phase transition is one main particle source of stochastic gravitational wave (GW) background to be observed in the future GW observatories. Phase transition associated with the spontaneous symmetry breaking of Grand Unified Theories (GUTs) happens at an untouchable high energy scale. The GUT monopole problem requires that the GUT phase transition should happen before or during inflation. In this work, we assume the GUT phase transition happens during inflation. It solves the GUT monopole problem on one hand. On the other hand, GWs from GUT phase transition, if it is first-order, can be redshifted and deformed, and might be observed today in GW observatories. Different from some well-known GUT inflationary models where the GUT symmetry breaking is complete at the end of the inflation, we assume the phase transition proceeds very fast at some point during the inflation. The e-folding number of the phase transition is denoted as N_* . We study the general behaviour of the inflated GW spectrum and its application in GUT phase transition during inflation.

We derived the general formalism of GW spectrum generated from any instant source during inflation. The general correlation between the inflated and uninflated (i.e., GWs generated after inflation) GW spectra is given in Eq. (2.28). Beside the redshift of frequency, another important modification of the GW spectrum is the deformation. It changes the shape of spectrum. We denote the deformation function as $S(f)$ with f the frequency to-

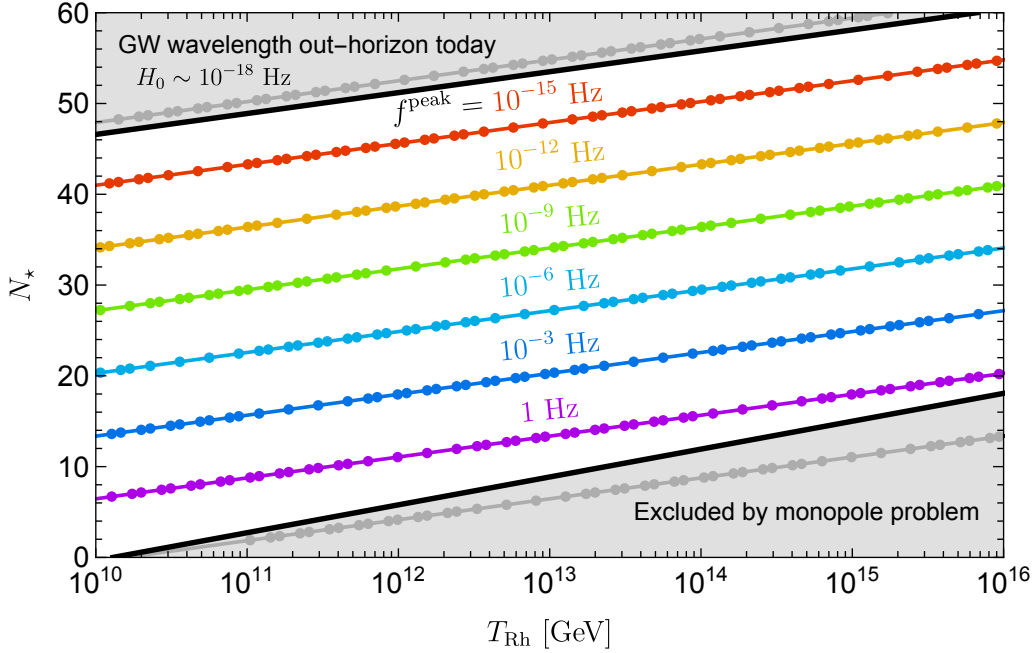


Figure 7. The dependence of the peak frequency f^{peak} of the inflated GW spectrum on the reheating temperature T_{Rh} and the e-folding number N_* at the phase transition. Values of the parameters $\rho_{\text{PT}}/\rho_{\text{tot}} = 0.1$, $\beta/H_* = 5$ and $v_w = 1$ are taken. The grey region in the bottom-right corner is the excluded region in solving the monopole problem, where the monopole mass is assumed to be at the same scale of the reheating temperature. That in the top-left corner is that the wavelength of GW is outside the horizon today.

day. We give a complete analytical description of the deformation function for the e-folding number N_* taking any reasonable value $0 < N_* \lesssim 60$. For $N_* > 5$, we recover the result obtained in [25]. We clarified IR and UV regimes by comparing the frequency nowadays f with $\frac{a_* H_*}{2\pi a_0}$, and $f \gg \frac{a_{\text{Rh}} H_*}{2\pi a_0}$ is further regarded as the FUV regime. Properties of the deformation function in these regimes were discussed. Here, a_* , a_{Rh} , and a_0 are co-moving factors at instant source, at reheating, and today, respectively, and H_* is the Hubble rate at instant source, which is identical to the Hubble rate during inflation. In the IR band, the deformation is frequency-independent, providing only an overall suppression factor $1/9$ for $N_* > 5$. In the UV band, $S(f)$ oscillates along f . In the FUV band, $S(f)$ provides an suppression inversely proportional to the quartic square of the co-moving factor.

We apply the formalism to GUT phase transition during inflation. The instant-source approximation holds with the assumption $\beta/H_* > 5$, where β is the inverse duration of phase transition. The inflated GW spectrum, after deformed by inflation, shows the peak of the spectrum at $f^{\text{peak}} \simeq 60 \text{ MHz} \cdot \left(\frac{T_{\text{Rh}}}{10^{15} \text{ GeV}}\right) e^{-N_*}$ and the peak amplitude highly suppressed by a factor $\sim (\beta/H_*)^{-5}$. This peak is not simply a redshift of the peak of uninflated GW spectrum obtained by phase transition in the radiation era. For $N_* \simeq 15$ and 25 , inflation pushes the peak frequency of GWs from 0.1 GHz to 10 Hz and mHz hands, respectively, referring to the favoured regimes for ground-based and space-based laser interferometers,

respectively. LISA/Taiji will be able to test GUT phase transition with $\rho_{\text{PT}}/\rho_{\text{tot}} \sim \mathcal{O}(0.1)$ and $\beta/H_\star \lesssim 10$. The best sensitivity of GW measurements in the foreseeable future may be able to test $\rho_{\text{PT}}/\rho_{\text{tot}} \approx \mathcal{O}(10^{-4})$ or $\beta/H_\star \lesssim 40$. A larger e-folding number $N_\star \simeq 36$ can further push the GWs to the nHz band, but the suppressed amplitude cannot explain the hint of PTA data. We further generalised the discussion to inflated GWs via phase transition below the GUT scale by relaxing the reheating temperature.

Acknowledgments

Y.L.Z. would like to thank useful discussion with H.P. An. This work was supported by the National Natural Science Foundation of China (NSFC) under Grant Nos. 12205064, 12347103, and Zhejiang Provincial Natural Science Foundation of China under Grant No. LDQ24A050002.

References

- [1] A. M. Polyakov, JETP Lett. **20** (1974), 194-195 PRINT-74-1566 (LANDAU-INST).
- [2] G. 't Hooft, Nucl. Phys. B **79** (1974), 276-284 doi:10.1016/0550-3213(74)90486-6
- [3] A. H. Guth, Phys. Rev. D **23** (1981), 347-356 doi:10.1103/PhysRevD.23.347
- [4] A. D. Linde, Phys. Lett. B **108** (1982), 389-393 doi:10.1016/0370-2693(82)91219-9
- [5] A. Albrecht and P. J. Steinhardt, Phys. Rev. Lett. **48** (1982), 1220-1223 doi:10.1103/PhysRevLett.48.1220
- [6] S. F. King, S. Pascoli, J. Turner and Y. L. Zhou, Phys. Rev. Lett. **126** (2021) no.2, 021802 doi:10.1103/PhysRevLett.126.021802 [arXiv:2005.13549 [hep-ph]].
- [7] J. A. Dror, T. Hiramatsu, K. Kohri, H. Murayama and G. White, Phys. Rev. Lett. **124** (2020) no.4, 041804 doi:10.1103/PhysRevLett.124.041804 [arXiv:1908.03227 [hep-ph]].
- [8] S. F. King, S. Pascoli, J. Turner and Y. L. Zhou, JHEP **10** (2021), 225 doi:10.1007/JHEP10(2021)225 [arXiv:2106.15634 [hep-ph]].
- [9] S. Bertolini, L. Di Luzio and M. Malinsky, Phys. Rev. D **80** (2009), 015013 doi:10.1103/PhysRevD.80.015013 [arXiv:0903.4049 [hep-ph]].
- [10] J. Chakraborty, R. Maji and S. F. King, Phys. Rev. D **99** (2019) no.9, 095008 doi:10.1103/PhysRevD.99.095008 [arXiv:1901.05867 [hep-ph]].
- [11] D. Meloni, T. Ohlsson and M. Pernow, Eur. Phys. J. C **80** (2020) no.9, 840 doi:10.1140/epjc/s10052-020-8308-9 [arXiv:1911.11411 [hep-ph]].
- [12] S. Antusch, K. Hinze, S. Saad and J. Steiner, Phys. Rev. D **108** (2023) no.9, 095053 doi:10.1103/PhysRevD.108.095053 [arXiv:2307.04595 [hep-ph]].
- [13] W. Buchmuller, V. Domcke, H. Murayama and K. Schmitz, Phys. Lett. B **809** (2020), 135764 doi:10.1016/j.physletb.2020.135764 [arXiv:1912.03695 [hep-ph]].
- [14] W. Buchmuller, V. Domcke and K. Schmitz, Phys. Lett. B **811** (2020), 135914 doi:10.1016/j.physletb.2020.135914 [arXiv:2009.10649 [astro-ph.CO]].
- [15] W. Buchmuller, V. Domcke and K. Schmitz, JCAP **12** (2021) no.12, 006 doi:10.1088/1475-7516/2021/12/006 [arXiv:2107.04578 [hep-ph]].

- [16] M. A. Masoud, M. U. Rehman and Q. Shafi, JCAP **11** (2021), 022
doi:10.1088/1475-7516/2021/11/022 [arXiv:2107.09689 [hep-ph]].
- [17] B. Fu, S. F. King, L. Marsili, S. Pascoli, J. Turner and Y. L. Zhou, Phys. Rev. D **109** (2024) no.5, 5 doi:10.1103/PhysRevD.109.055025 [arXiv:2308.05799 [hep-ph]].
- [18] G. Lazarides, R. Maji, A. Moursy and Q. Shafi, JCAP **03** (2024), 006
doi:10.1088/1475-7516/2024/03/006 [arXiv:2308.07094 [hep-ph]].
- [19] S. F. King, G. K. Leontaris and Y. L. Zhou, JHEP **03** (2024), 006
doi:10.1007/JHEP03(2024)006 [arXiv:2311.11857 [hep-ph]].
- [20] D. Croon, T. E. Gonzalo and G. White, JHEP **02** (2019), 083 doi:10.1007/JHEP02(2019)083 [arXiv:1812.02747 [hep-ph]].
- [21] W. C. Huang, F. Sannino and Z. W. Wang, Phys. Rev. D **102** (2020) no.9, 095025
doi:10.1103/PhysRevD.102.095025 [arXiv:2004.02332 [hep-ph]].
- [22] P. Athron, C. Balázs, T. E. Gonzalo and M. Pearce, Phys. Rev. D **109** (2024) no.6, L061303
doi:10.1103/PhysRevD.109.L061303 [arXiv:2307.02544 [hep-ph]].
- [23] V. Brdar, L. Graf, A. J. Helmboldt and X. J. Xu, JCAP **12** (2019), 027
doi:10.1088/1475-7516/2019/12/027 [arXiv:1909.02018 [hep-ph]].
- [24] M. Li, Q. S. Yan, Y. Zhang and Z. Zhao, JHEP **03** (2021), 267
doi:10.1007/JHEP03(2021)267 [arXiv:2012.13686 [hep-ph]].
- [25] H. An, K. F. Lyu, L. T. Wang and S. Zhou, Chin. Phys. C **46** (2022) no.10, 101001
doi:10.1088/1674-1137/ac76a7 [arXiv:2009.12381 [astro-ph.CO]].
- [26] H. An, K. F. Lyu, L. T. Wang and S. Zhou, JHEP **06** (2022), 050
doi:10.1007/JHEP06(2022)050 [arXiv:2201.05171 [astro-ph.CO]].
- [27] H. An, B. Su, H. Tai, L. T. Wang and C. Yang, Phys. Rev. D **109** (2024) no.12, L121304
doi:10.1103/PhysRevD.109.L121304 [arXiv:2308.00070 [astro-ph.CO]].
- [28] Q. Shafi and A. Vilenkin, Phys. Rev. Lett. **52** (1984), 691-694
doi:10.1103/PhysRevLett.52.691
- [29] G. Lazarides and C. Panagiotakopoulos, Phys. Rev. D **52** (1995), R559-R563
doi:10.1103/PhysRevD.52.R559 [arXiv:hep-ph/9506325 [hep-ph]].
- [30] C. Caprini, M. Hindmarsh, S. Huber, T. Konstandin, J. Kozaczuk, G. Nardini, J. M. No, A. Petiteau, P. Schwaller and G. Servant, *et al.* JCAP **04** (2016), 001
doi:10.1088/1475-7516/2016/04/001 [arXiv:1512.06239 [astro-ph.CO]].
- [31] A. Kosowsky, M. S. Turner and R. Watkins, Phys. Rev. D **45** (1992), 4514-4535
doi:10.1103/PhysRevD.45.4514
- [32] A. Kosowsky, M. S. Turner and R. Watkins, Phys. Rev. Lett. **69** (1992), 2026-2029
doi:10.1103/PhysRevLett.69.2026
- [33] A. Kosowsky and M. S. Turner, Phys. Rev. D **47** (1993), 4372-4391
doi:10.1103/PhysRevD.47.4372 [arXiv:astro-ph/9211004 [astro-ph]].
- [34] M. Kamionkowski, A. Kosowsky and M. S. Turner, Phys. Rev. D **49** (1994), 2837-2851
doi:10.1103/PhysRevD.49.2837 [arXiv:astro-ph/9310044 [astro-ph]].
- [35] S. J. Huber and T. Konstandin, JCAP **09** (2008), 022 doi:10.1088/1475-7516/2008/09/022 [arXiv:0806.1828 [hep-ph]].

- [36] C. Caprini, R. Durrer, T. Konstandin and G. Servant, Phys. Rev. D **79** (2009), 083519 doi:10.1103/PhysRevD.79.083519 [arXiv:0901.1661 [astro-ph.CO]].
- [37] R. G. Cai, S. Pi and M. Sasaki, Phys. Rev. D **102** (2020) no.8, 083528 doi:10.1103/PhysRevD.102.083528 [arXiv:1909.13728 [astro-ph.CO]].
- [38] P. Amaro-Seoane *et al.* [LISA], [arXiv:1702.00786 [astro-ph.IM]].
- [39] W. H. Ruan, Z. K. Guo, R. G. Cai and Y. Z. Zhang, Int. J. Mod. Phys. A **35** (2020) no.17, 2050075 doi:10.1142/S0217751X2050075X [arXiv:1807.09495 [gr-qc]].
- [40] J. Luo *et al.* [TianQin], Class. Quant. Grav. **33** (2016) no.3, 035010 doi:10.1088/0264-9381/33/3/035010 [arXiv:1512.02076 [astro-ph.IM]].
- [41] V. Corbin and N. J. Cornish, Class. Quant. Grav. **23** (2006), 2435-2446 doi:10.1088/0264-9381/23/7/014 [arXiv:gr-qc/0512039 [gr-qc]].
- [42] N. Seto, S. Kawamura and T. Nakamura, Phys. Rev. Lett. **87** (2001), 221103 doi:10.1103/PhysRevLett.87.221103 [arXiv:astro-ph/0108011 [astro-ph]].
- [43] A. Sesana, N. Korsakova, M. A. Sedda, V. Baibhav, E. Barausse, S. Barke, E. Berti, M. Bonetti, P. R. Capelo and C. Caprini, *et al.* Exper. Astron. **51** (2021) no.3, 1333-1383 doi:10.1007/s10686-021-09709-9 [arXiv:1908.11391 [astro-ph.IM]].
- [44] P. W. Graham *et al.* [MAGIS], [arXiv:1711.02225 [astro-ph.IM]].
- [45] Y. A. El-Neaj *et al.* [AEDGE], EPJ Quant. Technol. **7** (2020), 6 doi:10.1140/epjqt/s40507-020-0080-0 [arXiv:1908.00802 [gr-qc]].
- [46] L. Badurina, E. Bentine, D. Blas, K. Bongs, D. Bortoletto, T. Bowcock, K. Bridges, W. Bowden, O. Buchmueller and C. Burrage, *et al.* JCAP **05** (2020), 011 doi:10.1088/1475-7516/2020/05/011 [arXiv:1911.11755 [astro-ph.CO]].
- [47] B. Sathyaprakash, M. Abernathy, F. Acernese, P. Ajith, B. Allen, P. Amaro-Seoane, N. Andersson, S. Aoudia, K. Arun and P. Astone, *et al.* Class. Quant. Grav. **29** (2012), 124013 [erratum: Class. Quant. Grav. **30** (2013), 079501] doi:10.1088/0264-9381/29/12/124013 [arXiv:1206.0331 [gr-qc]].
- [48] B. P. Abbott *et al.* [LIGO Scientific], Class. Quant. Grav. **34** (2017) no.4, 044001 doi:10.1088/1361-6382/aa51f4 [arXiv:1607.08697 [astro-ph.IM]].
- [49] G. Janssen, G. Hobbs, M. McLaughlin, C. Bassa, A. T. Deller, M. Kramer, K. Lee, C. Mingarelli, P. Rosado and S. Sanidas, *et al.* PoS **AASKA14** (2015), 037 doi:10.22323/1.215.0037 [arXiv:1501.00127 [astro-ph.IM]].
- [50] A. Afzal *et al.* [NANOGrav], Astrophys. J. Lett. **951** (2023) no.1, L11 [erratum: Astrophys. J. Lett. **971** (2024) no.1, L27; erratum: Astrophys. J. **971** (2024) no.1, L27] doi:10.3847/2041-8213/acdc91 [arXiv:2306.16219 [astro-ph.HE]].
- [51] R. Abbott *et al.* [LIGO Scientific, Virgo and KAGRA], Phys. Rev. Lett. **126** (2021) no.24, 241102 doi:10.1103/PhysRevLett.126.241102 [arXiv:2101.12248 [gr-qc]].
- [52] R. Jeannerot, S. Khalil, G. Lazarides and Q. Shafi, JHEP **10** (2000), 012 doi:10.1088/1126-6708/2000/10/012 [arXiv:hep-ph/0002151 [hep-ph]].
- [53] R. Jeannerot, J. Rocher and M. Sakellariadou, Phys. Rev. D **68** (2003), 103514 doi:10.1103/PhysRevD.68.103514 [arXiv:hep-ph/0308134 [hep-ph]].